Chemical and mechanical stimuli act on common signal transduction and cytoskeletal networks

Yulia Artemenko[a,1,2], Lucas Axiotakis Jr.[a], Jane Borleis[a], Pablo A. Iglesias[b], and Peter N. Devreotes[a,2]

[a]Department of Cell Biology, The Johns Hopkins University School of Medicine, Baltimore, MD 21205; and [b]Department of Electrical and Computer Engineering, Johns Hopkins University, Baltimore, MD 21218

Contributed by Peter N. Devreotes, October 6, 2016 (sent for review June 1, 2016; reviewed by Paul Kubes and Carole A. Parent)

Signal transduction pathways activated by chemoattractants have been extensively studied, but little is known about the events mediating responses to mechanical stimuli. We discovered that acute mechanical perturbation of cells triggered transient activation of all tested components of the chemotactic signal transduction network, as well as actin polymerization. Similarly to chemoattractants, the shear flow-induced signal transduction events displayed features of excitability, including the ability to mount a full response irrespective of the length of the stimulation and a refractory period that is shared with that generated by chemoattractants. Loss of G protein subunits, inhibition of multiple signal transduction events, or disruption of calcium signaling attenuated the response to acute mechanical stimulation. Unlike the response to chemoattractants, an intact actin cytoskeleton was essential for reacting to mechanical perturbation. These results taken together suggest that chemotactic and mechanical stimuli trigger activation of a common signal transduction network that integrates external cues to regulate cytoskeletal activity and drive cell migration.

biochemical excitability | shear stress | motility | biomechanics | inflammation

Migration of eukaryotic cells is guided by a number of chemical and physical cues in their environment. Chemotaxis, which refers to migration up a gradient of soluble chemoattractant, is by far the best understood mode of directed cell migration. However, cells can also be guided by gradients of substrate-bound chemoattractants (haptotaxis), variable stiffness of the substrates (durotaxis), electric fields (electrotaxis or galvanotaxis), or shear flow (rheotaxis). These different modes of directed migration have been implicated in diverse physiological and pathophysiological processes, including embryogenesis, wound healing, chronic inflammatory diseases, and cancer metastasis (1–3). Importantly, cell migration in vivo undoubtedly involves integration of multiple different signals.

In contrast to chemotaxis, thorough understanding of the signaling mechanisms that drive various other modes of directed migration is lacking. Similarly to chemotaxing cells, several studies have reported activation and/or localization of typical leading edge markers, including actin polymerization, phosphatidylinositol 3,4,5-trisphosphate (PIP3), and/or extracellular signal-regulated kinase (ERK) 1/2, at the front of cells undergoing either shear-flow–mediated migration or electrotaxis (4–7). However, these activities were observed under steady-state conditions and, because these activities are associated with random projections, their appearance at the leading edge most likely merely reflects the abundance of projections at the front induced by mechanical or electrical forces.

Much of our understanding of the regulatory mechanisms in chemotaxis comes from studies of the social amoeba *Dictyostelium discoideum*. Efficient chemotaxis relies on the integration of motility, directional sensing, and polarity. These behaviors can be described in terms of receptor/G protein, signal transduction, cytoskeletal, and polarity networks. Chemoattractant binding to its G-protein–coupled receptor transmits the signal via heterotrimeric G proteins to the downstream signal transduction network, which amplifies the directional signal. Multiple pathways within the signal transduction network act in parallel to bias actin polymerization, and consequent pseudopod protrusion, in the direction of the gradient. Feedback mechanisms within the signal transduction network together with cell polarity further amplify the response. Important parts of this paradigm have been substantiated in other cells that undergo rapid amoeboid-type migration, including neutrophils and metastatic cancer cells (3).

Until recently, random cell migration was thought to exclusively involve the activity of the actin cytoskeleton, which is biased in the presence of chemoattractants by the G protein and signal transduction networks. However, evidence is accumulating to favor the view that both the signal transduction and actin cytoskeleton networks are required for random motility. In the absence of signal transduction, rapid cytoskeletal oscillations cause undulations only on the cell perimeter (8, 9). Larger protrusions, which drive cell migration, require local spontaneous triggering of an excitable signal transduction network to organize the cytoskeleton. Further supporting this coupling scheme is the observation that most chemotaxis mutants affect signal transduction and have impaired random migration.

The signal transduction–cytoskeletal coupling model suggests that diverse guidance cues might converge on a common signal transduction network that drives random cell migration. A serendipitous discovery that *Dictyostelium* cells display biochemical responses to acute mechanical force allowed us to test this hypothesis. Shear flow triggered rapid and transient activation of every pathway we examined across the chemotactic signal transduction network. Moreover, it appears that shear stress and chemoattractants activate the same excitable signal transduction

Significance

Cells directionally migrate in response to a variety of external cues, including chemical, electrical, and mechanical stimuli; however, only response to chemoattractants has been characterized at the molecular level. Binding of chemoattractants to specific surface receptors triggers rapid, transient activation of many signal transduction and cytoskeletal events. We discovered that brief application of shear stress to cells likely elicits activation of all of the same events. Responses to chemoattractants and shear stress are susceptible to many of the same perturbations, although that to mechanical stimulation uniquely is blocked by disruption of the actin cytoskeleton. Our finding provides insight into the molecular mechanism of cellular response to mechanical stimuli and has important implications for integration of chemical and mechanical inputs.

Author contributions: Y.A. and P.N.D. designed research; Y.A., L.A., and J.B. performed research; P.A.I. contributed new reagents/analytic tools; Y.A. and L.A. analyzed data; and Y.A. and P.N.D. wrote the paper.

Reviewers: P.K., University of Calgary, Faculty of Medicine; and C.A.P., National Cancer Institute, NIH.

The authors declare no conflict of interest.

[1]Present address: Department of Biological Sciences, SUNY Oswego, Oswego, NY 13126.

[2]To whom correspondence may be addressed. Email: pnd@jhmi.edu or yulia.artemenko@oswego.edu.

This article contains supporting information online at www.pnas.org/lookup/suppl/doi:10.1073/pnas.1608767113/-/DCSupplemental.

network, allowing for interaction and/or integration of the two processes.

Results

Acute Mechanical Stimulation Triggers Activation of Multiple Branches of the Chemotactic Signal Transduction Network. In the course of an experiment designed to monitor signal transduction responses, we discovered that applying acute shear stress for just 5 s to adherent aggregation-competent *Dictyostelium* cells led to transient phosphorylation of kinases PKBR1, ERK2, and KrsB with the timing typically observed for chemoattractant-induced stimulation (Fig. 1*A* and Fig. S1*A*). PKBR1 and KrsB phosphorylation peaked at 10–15 s, whereas ERK2 was maximally phosphorylated around 30 s poststimulation. Acute shear stress also activated PKBA, although this response was dampened due to the presence of caffeine (Fig. S1*A*).

To observe the effect of acute mechanical stimulation on individual cell behavior, we analyzed localization of several biosensors in cells following a brief pulse of unidirectional laminar flow in a perfusion chamber. Typical "front" markers, such as $LimE_{\Delta coil}$, which detects newly polymerized actin, and the PIP3 sensor PH-Crac transiently translocated from the cytosol to the cortex, peaking around 9 s poststimulation (Fig. 1 *B* and *C* and Movie S1). Biosensors for activated Ras (RBD) and Rap1 (RalGDS) also showed similar behavior (Fig. S1 *B* and *C*). In contrast, "back" markers phosphatase and tensin homolog (PTEN) and Callipygian (CynA) showed opposite localization with slightly delayed timing, with the highest accumulation in the cytosol observed at 15–18 s (Fig. 1 *D* and *E* and Movie S1). Although most of the cells showed a $LimE_{\Delta coil}$, PH-Crac, PTEN, or CynA response, the magnitude of the response differed among the cells (Fig. 1 *F* and *G* and Fig. S1 *D* and *E*). Thus, brief application of shear stress triggers actin polymerization, as well as activation of multiple branches of the chemotactic signal transduction network.

Stimulation of vegetative cells with a brief pulse of unidirectional laminar flow in the perfusion chamber also led to robust actin polymerization and Ras activation at the cell cortex, with a peak around 6 s poststimulation (Fig. 2*A* and Movie S2). Importantly, $LimE_{\Delta coil}$ recruitment to the cell cortex in response to acute mechanical stimulation was not due to shear-induced cell migration (Fig. 2*B*). In fact, cells transiently stalled following acute mechanical stimulation, as evidenced by the significant

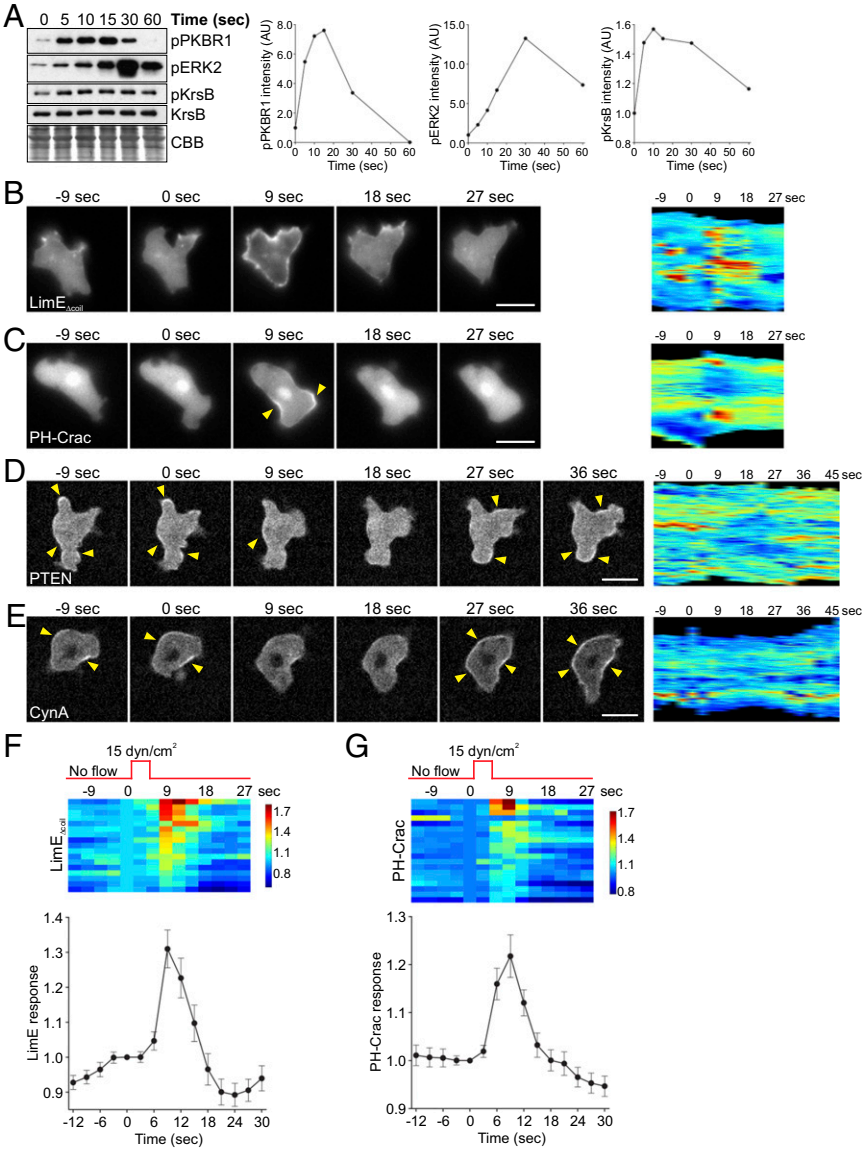

Fig. 1. Acute mechanical stimulation activates multiple signal transduction pathways. (*A*) Aggregation-competent WT cells were stimulated on a rotary shaker for 5 s, lysed at the indicated time points, and immunoblotted using antibodies that recognize phosphorylated PKBR1, ERK2, and KrsB, as well as total KrsB. The membrane was stained with Coomassie Brilliant Blue (CBB) to show equal protein loading. The mean intensity of the phosphorylated bands was normalized for the intensity of the corresponding total KrsB bands and plotted against time. Another example of the time course of protein phosphorylation in response to acute mechanical stimulation is shown in Fig. S1*A*. (*B*–*G*) Aggregation-competent WT cells expressing various fluorescently tagged biosensors were stimulated with unidirectional laminar flow at 15 dyn/cm^2 (*B*–*D*) or 21 dyn/cm^2 (*E*) for 2–5 s. Images were collected every 3 s. (*B*–*E*) A representative cell showing translocation of $LimE_{\Delta coil}$ (*B*), PH-Crac (*C*), PTEN (*D*), and CynA (*E*) in response to mechanical stimulation. A kymograph showing changes in the cortical signal along the entire cell perimeter (shown as a vertical line) with time is shown for each cell. Arrowheads point to areas of biosensor accumulation at the cortex. (*F* and *G*) $LimE_{\Delta coil}$ (*F*) or PH-Crac (*G*) accumulation at the cortex was quantified as the inverse of the mean cytoplasmic intensity normalized for time 0. Responses of individual cells are represented as rows on a heat map. The average response of 18 (*F*) or 20 (*G*) cells is shown at *Bottom*. Values are mean ± SE. Similar analysis of PTEN and CynA is shown in Fig. S1 *D* and *E*. (Scale bar, 10 μm.)

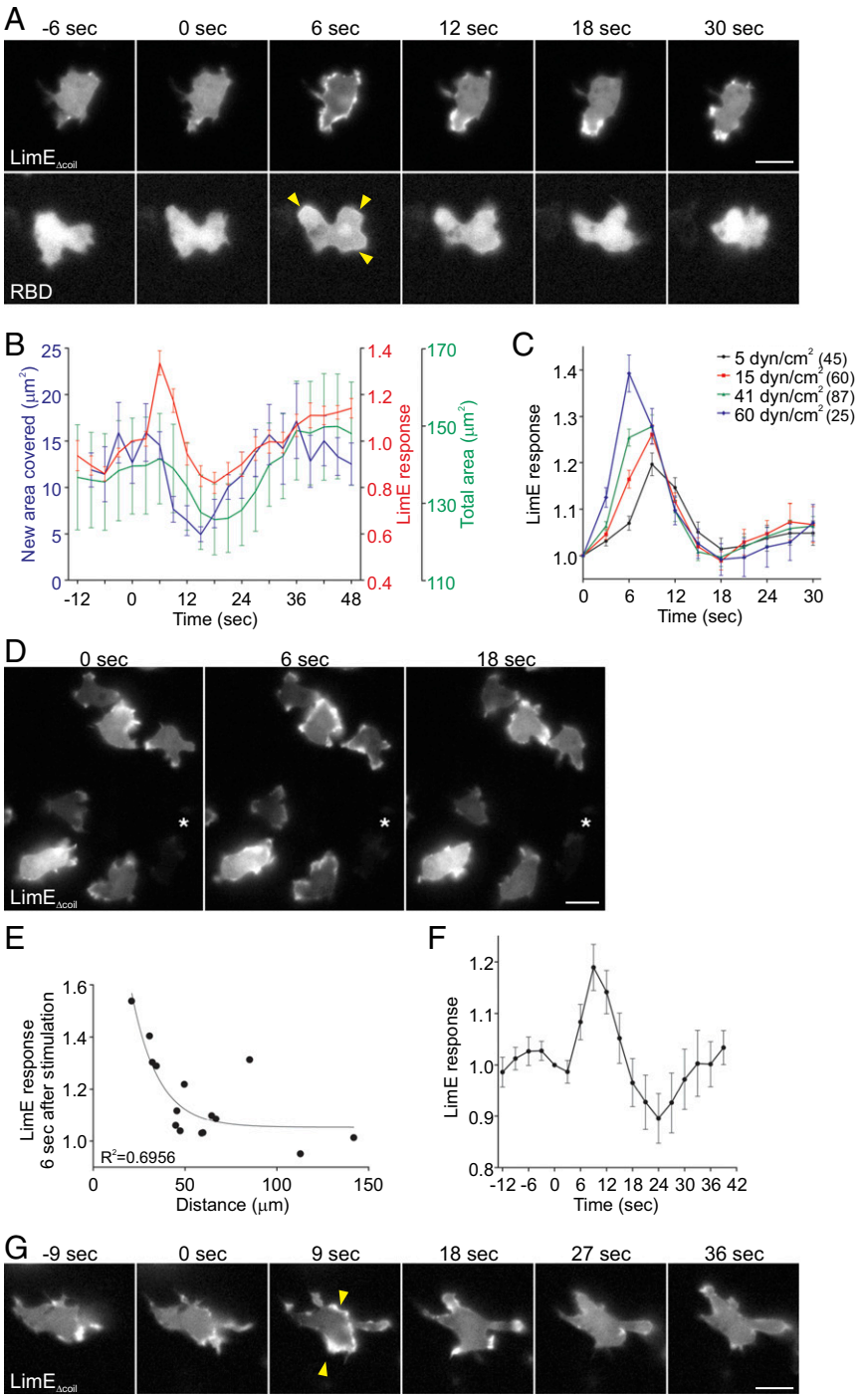

Fig. 2. Response to shear flow is due to mechanical perturbation and not to soluble factors. (*A* and *B*) Vegetative WT cells expressing LimE$_{\Delta coil}$-RFP or RBD-GFP were stimulated with unidirectional laminar flow at 41 dyn/cm^2 for 2 s. Images were collected every 3 s. Representative images are shown in *A*. (*B*) LimE$_{\Delta coil}$-RFP accumulation at the cortex was quantified as in Fig. 1*F*. New area occupied by the cell was calculated using the number of new pixels covered by a cell in consecutive frames. Values are mean ± SE of 8 cells. (C) Vegetative WT cells expressing LimE$_{\Delta coil}$-RFP were stimulated at the indicated shear stress values, imaged, and analyzed as in *B*. The number of cells analyzed is indicated beside each condition. (*D*) Vegetative WT cells expressing LimE$_{\Delta coil}$-RFP were exposed to a micropipette that provided a background flow of the assay buffer. At time 0, a brief bolus of assay buffer was delivered, after which the cells were returned to the background flow rate condition. Images were collected every 3 s. (*E*) Peak LimE$_{\Delta coil}$-RFP accumulation at the cortex following stimulation in *D* for 15 individual cells was plotted against the distance between the cell centroid and the tip of the micropipette. Peak accumulation was quantified as the inverse of the mean cytoplasmic intensity 6 s after the start of stimulation, normalized for time 0. The trendline represents a fit to a one-phase decay. (*F* and *G*) Vegetative WT cells expressing LimE$_{\Delta coil}$-RFP were imaged under constant shear flow at ~5 dyn/cm^2. At time 0, the shear stress was increased to ~60 dyn/cm^2 for 5 s by transiently increasing the flow rate. (*F*) LimE$_{\Delta coil}$-RFP accumulation at the cortex was quantified as in Fig. 1*F*. Values are mean ± SE of 20 cells. Arrowheads point to areas of biosensor accumulation at the cortex. A representative cell is shown in *G*. (Scale bar, 10 μm.)

reduction in the formation of new protrusions between 9 and 18 s poststimulation ($P < 0.05$ between 9 and 18 s by paired t test compared with time 0). LimE$_{\Delta coil}$ response was also followed by a slight transient decrease in the total area of the cell between 15 and 21 s, similarly to the "cringe" that follows stimulation with a chemoattractant, and a spreading response between 36 and 45 s, corresponding to cells resuming migration ($P < 0.05$ at the specified time points by paired t test compared with time 0). The latter phase also correlated with an increase in the LimE$_{\Delta coil}$ signal at the cortex due to its accumulation on the newly formed protrusions. Continuous stimulation of vegetative *Dictyostelium* cells with unidirectional laminar flow also resulted in a transient LimE$_{\Delta coil}$ response followed by a polarized response and migration against the flow ~2 min after the induction of flow (Fig. S2 *A* and *B* and Movie S3). Sensitivity to mechanical perturbation appears to be a conserved behavior in eukaryotic cells, because acute stimulation of human neutrophil-like HL-60 cells with shear flow also resulted in a spreading response where the cells appear phase dark ~1–2 min after stimulation ($P < 0.05$ at 60 s; Fig. S2*C* and Movie S4). The transient spreading response was also observed following continuous exposure to shear flow (Movie S4).

The response of individual cells measured by LimE$_{\Delta coil}$ translocation, as well as the response of a cell population measured by PKBR1 phosphorylation increased with the amount of unidirectional shear stress applied (Fig. 2*C*, Fig. S2*D*, and Movie S5).

Similarly, when cells were exposed to an increase in shear stress delivered by a micropipette filled with the assay buffer, the cells in the vicinity showed transient $LimE_{\Delta coil}$ recruitment to the cell cortex (Fig. 2*D*). The response was inversely correlated with the distance of the cell to the micropipette, again suggesting that it depended on the level of applied shear (Fig. 2*E*).

Several controls suggested that the responses were dependent on the mechanical perturbation. First, they did not depend on the chemoattractant cAMP because cells lacking adenylyl cyclase or cAMP receptors 1 and 3, which cannot produce or respond to cAMP, respectively, were still able to polymerize actin following acute mechanical stimulation with shear flow (Fig. S2 *E–I*). Second, several observations suggested that these responses did not depend on the accumulation of other soluble factors in the assay buffer: (*i*) When we stimulated cells that were already under perfusion, a transient increase in the flow rate, which elevated shear stress from 5 to 60 dyn/cm^2, triggered robust actin polymerization at the cell cortex (Fig. 2 *F* and *G* and Movie S6). (*ii*) In the micropipette experiments described above there was basal flow from the micropipette before the stimulus. Furthermore, as shown below, cells responded repeatedly to brief increases in shear stress spaced only 45 s apart.

Response to Acute Mechanical Stimulation Has Characteristics of an Excitable System. Because mechanical stimulation and chemoattractants trigger activation of the same signal transduction network, responses to mechanical stimulation might be expected to be excitable in nature, similarly to chemoattractant-induced responses. Two features of excitable systems that are seen for chemoattractants are the all-or-none nature of the response, as well as the presence of a refractory period. When we tested response to a 2-s or 10-s pulse at low shear stress values, we saw an increase in $LimE_{\Delta coil}$ recruitment with longer stimulus duration (Fig. 3*A*). However, at high shear stress, the peak response to a 2-s stimulation was not significantly different from a 10-s stimulation (Fig. 3*A*), similarly to the full response observed following either brief or prolonged stimulation with saturating amounts of chemoattractant (8).

To assess the refractory period of the response to mechanical stimulation, we subjected cells to consecutive 2-s stimuli at 41 dyn/cm^2, varying the interval between the two from 12 to 45 s (Fig. 3 *B* and *C*, Fig. S3*A*, and Movie S7). Under these conditions, response to the second stimulus was absent when the interval was less than 12 s, corresponding to an absolute refractory period. Thereafter, the response recovered with a half-time of ~7 s, as observed for chemoattractant-induced stimulation (8). The response was fully recovered when the interval was 45 s.

Finally, to assess whether refractoriness to mechanical and chemotactic stimuli involve the same process, cells were exposed to a mechanical stimulus, delivered by a bolus addition of buffer and then to uniform folic acid (Fig. 3*D*, Fig. S3 *B* and *C*, and Movie S8). When the interval between the two stimuli was 45 s, the response to 20 nM folic acid was similar to a response with no prior stimulation. In contrast, when the interval between mechanical and chemical stimulation was 12 s, the integrated response to folic acid was diminished by over 60%. Thus, mechanical and chemoattractant stimulation appear to share the refractory process.

Role of the Signal Transduction Network in the Response to Acute Mechanical Stimulation. To determine whether the signal transduction network that is activated by mechanical stimulation is necessary for the cell to transmit the stimulus, we examined the behavior of cells with disrupted single or multiple signal transduction pathways. Treatment of cells with LY294002, which inhibits PI3K, had no effect on their ability to recruit $LimE_{\Delta coil}$ following a brief exposure to shear flow (Fig. 4*A* and Fig. S4*A*). Previous studies reported that disruption of four pathways (PI3K, TORC2, PLA_2, and sGC) simultaneously abolishes chemotactic responses (10, 11). In our hands, these cells were able to recruit $LimE_{\Delta coil}$ following a brief pulse of flow, although the response was significantly reduced compared with cells lacking one (sGC) or two (sGC and PI3K) pathways (Fig. 4*B*, Fig. S4*B*, and Movie S9). For cells lacking sGC, PLA_2, and TORC2 pathways, which had the least robust response to mechanical stimulation, there was also an apparent lack of shut-off following a response, although this was not the case for cells lacking PI3K activity as well. It is possible that the slow recovery of *sGC/pla$_2$/pia*$^-$ is due to increased basal activity of these cells because they appeared to have more macropinosomes than other double- or triple-null cells. Consistently, inhibition of the PI3K pathway, which has been previously shown to be important for macropinosome formation (12), appeared to slightly improve the profile of the response in these cells.

Next we tested whether perturbations that affect the response to mechanical stimulation also alter motility because this is a prediction that can be made from the coupling model where the signal transduction and cytoskeletal networks act together to induce formation of protrusions. Indeed, the ability of cells with a disrupted signal transduction pathway(s) to respond to mechanical stimulation correlated with their random migration. Cells lacking sGC, TORC2, and PLA_2 pathways, with or without PI3K signaling, had a significant reduction in migration speed (Fig. 4*C*, Movie S10, and Table S1). As mentioned above, the absence of PI3K activity slightly improved cell directionality likely due to the reduction in macropinosome formation (12). Overall, this finding suggests that acute mechanical stimulation might be acting on the same network that controls random activity and migration.

Fache et al. previously reported reduced shear-flow–induced motility for cells lacking G_β (13). Thus, we examined whether heterotrimeric G proteins are involved in the response to acute stimulation with shear flow. Cells that lack G_β (*gpbA*$^-$) or G_γ (*gpgA*$^-$) were extremely resistant to brief stimulation with flow, even at shear stress values higher than typically used for WT cells (60 compared with 41 dyn/cm^2; Fig. 4 *E* and *F* and Movie S11). We did observe $LimE_{\Delta coil}$ recruitment in *gpgA*$^-$ cells at higher shear stress values occasionally (Fig. 4 *E*, bottom row, and *F* and Movie S11). Expression of G_γ rescued the phenotype *gpgA*$^-$ cells. Similarly to cells lacking multiple signal transduction pathways, random migration of *gpbA*$^-$ *and gpgA*$^-$ cells was significantly impaired (Fig. 4*G*, Fig. S4*C*, Movie S12, and Table S2). In addition, consistent with previous studies (13), we also observed a reduction in shear-flow–induced migration of *gpbA*$^-$ and *gpgA*$^-$ cells (Fig. 4*G*, Fig. S4*C*, and Movie S12). Increasing the rate of shear flow improved directional migration of *gpbA*$^-$ cells (Fig. S4*C* and Table S2). It should be noted that WT cells migrated against shear flow at 10 dyn/cm^2, but switched their direction of migration to going with the flow at 25 dyn/cm^2 (Fig. S4*C*). In contrast, G-protein–null cells migrated with the flow even at 10 dyn/cm^2 (Fig. 4*G* and Fig. S4*C*).

Role of Calcium Flux in the Response to Acute Mechanical Stimulation. Because mechanosensation in a variety of cell types is accompanied by a burst in Ca^{2+} levels (14), we examined whether Ca^{2+} signaling plays a role in the response of *Dictyostelium* to acute mechanical stimulation. The standard buffer used in the experiments thus far was phosphate buffer supplemented with 2 mM $MgSO_4$ and 200 μM $CaCl_2$. When we assessed the responsiveness of developed cells in phosphate buffer without cation supplementation, we observed reduced phosphorylation of PKBR1 and ERK2 10 s following acute stimulation with shear flow on a rotary shaker (Fig. 5 *A* and *B*). The response was rescued by addition of 1 mM $CaCl_2$ or $MgCl_2$ (Fig. S5*A*). Growth stage cells are less sensitive to extracellular calcium, because there was

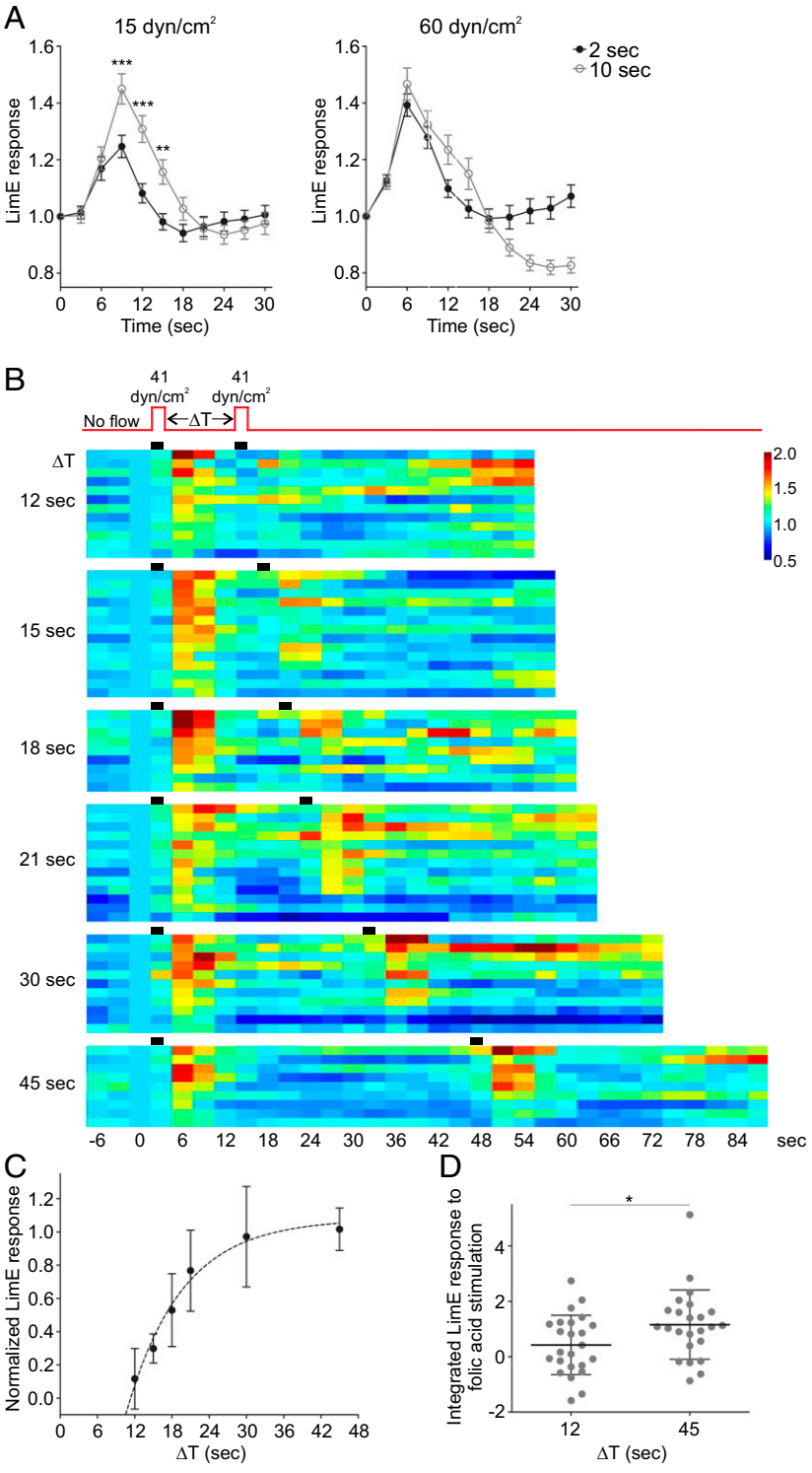

Fig. 3. Response to acute mechanical stimulation has characteristics of excitability. (*A*) Vegetative WT cells expressing $LimE_{\Delta coil}$-RFP were stimulated with unidirectional laminar flow at 15 or 60 dyn/cm^2 for 2 or 10 s. Images were collected every 3 s. $LimE_{\Delta coil}$-RFP accumulation at the cortex was quantified as in Fig. 1*F*. Values are mean ± SE of 40 and 34 cells for 15 dyn/cm^2 for 2 s and 10 s, and 25 and 30 cells for 60 dyn/cm^2 for 2 s and 10 s. (*B* and *C*) Vegetative WT cells expressing $LimE_{\Delta coil}$-RFP were stimulated with unidirectional laminar flow at 41 dyn/cm^2 twice, separated by varying delays (ΔT), and images were collected every 3 s. $LimE_{\Delta coil}$-RFP accumulation at the cortex was quantified as in Fig. 1*F*. Average values are shown in Fig. S3*A*. (*B*) The response of individual cells, represented as rows on a heat map, show cell-to-cell variations. (*C*) Average ratio of the peak response 6 s after the second stimulation to 6 s after the first stimulation was plotted against ΔT. Values are mean ± SE of 10–14 cells. The trendline is based on a one-phase decay function. (*D*) Vegetative WT cells expressing $LimE_{\Delta coil}$-RFP were first manually stimulated with shear flow; after a delay of 12 or 45 s, they were then stimulated with 20 nM folic acid. Images were collected every 3 s. $LimE_{\Delta coil}$-RFP accumulation at the cortex was quantified as the inverse of the mean cytoplasmic intensity normalized for time 0 of folic acid application and corrected for vehicle addition alone. The integrated response between 0 and 24 s after folic acid stimulation is shown. Horizontal lines and error bars represent mean ± SD, $^*P < 0.05$.

robust recruitment of $LimE_{\Delta coil}$ or RBD in phosphate or tricine buffer without cation supplementation in these cells (Fig. 5*C* and Fig. S5*B*). Addition of 1 mM $CaCl_2$ slightly improved the peak actin polymerization at the cortex following exposure to acute unidirectional laminar flow, and addition of $CaCl_2$ up to 10 mM did not further enhance the response. On the other hand, depletion of calcium with prolonged EGTA treatment significantly inhibited recruitment of $LimE_{\Delta coil}$ in these cells (Fig. 5*D* and Fig. S5*C*). Together these results suggest that vegetative cells have larger calcium stores than developed cells and thus are less susceptible to fluctuations in external calcium levels.

Because calcium flux can contribute to the response to a mechanical stimulus, there are likely channels that allow calcium influx either from the extracellular space and/or from internal stores. A recent study by Lima et al. examined the role of several putative cation channels in rheotaxis or shear-flow–induced cell migration, and implicated polycystin-like channel Pkd2, and to a smaller extent mucolipin (Mcln) in this process (15). In our assays

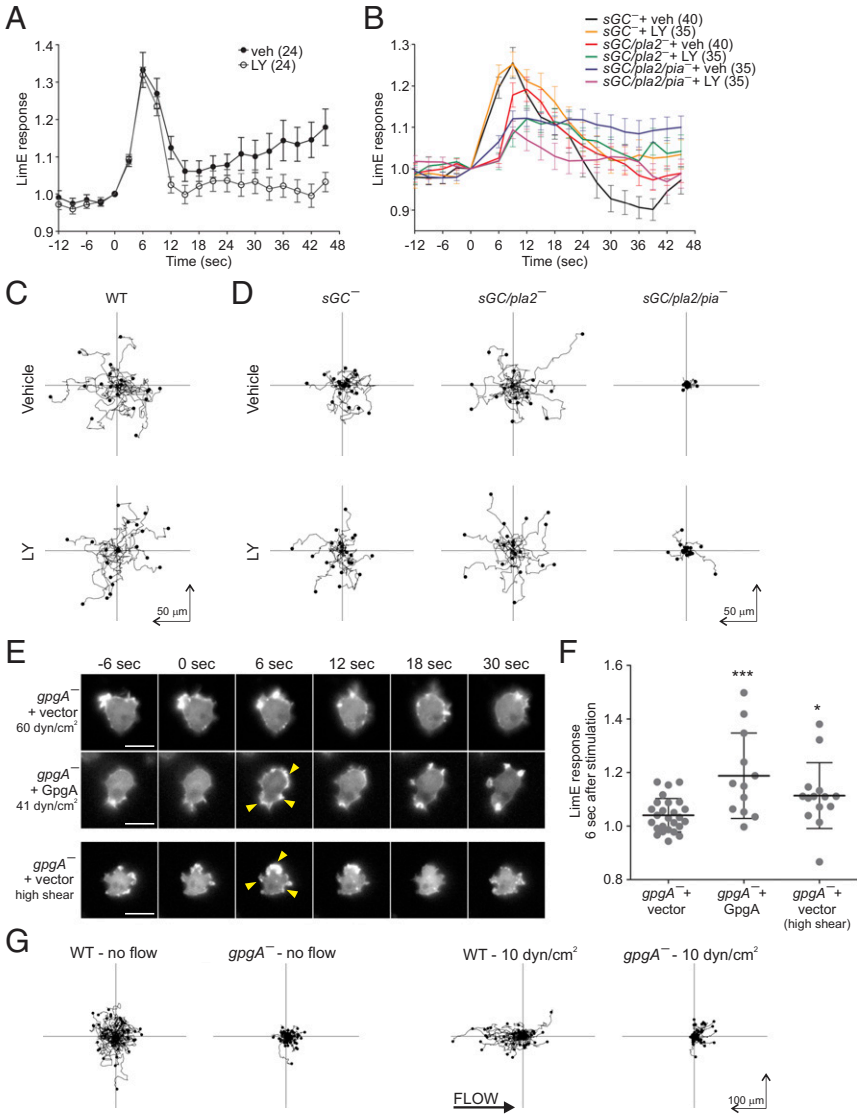

Fig. 4. Effect of inhibition of the signal transduction network and G proteins on the response to acute mechanical stimulation. (*A* and *B*) Vegetative WT cells (*A*), or *sGC*⁻, *sGC/pla2*⁻, and *sGC/pla2/pia*⁻ cells (*B*) expressing $LimE_{\Delta coil}$-RFP were treated with vehicle or 50 μM LY294002 for at least 30 min and then stimulated with unidirectional laminar flow at 41 dyn/cm² for 2 s. Images were collected every 3 s. $LimE_{\Delta coil}$-RFP accumulation at the cortex was quantified as in Fig. 1*F*. Values are mean ± SE. The number of cells analyzed is indicated beside each condition. Peak response values for individual cells are shown in Fig. S4 *A* and *B*. (*C* and *D*) Randomly migrating vegetative WT (*C*) or *sGC*⁻, *sGC/pla2*⁻, and *sGC/pla2/pia*⁻ (*D*) cells treated with vehicle or 50 μM LY294002 for 60 min were imaged every 20 s for 20 min. Tracks of 20 cells are shown. (*E* and *F*) Vegetative *gpgA*⁻ expressing vector or GpgA, as well as $LimE_{\Delta coil}$-RFP were stimulated with unidirectional laminar flow at the indicated pressure for 2 s. Images were collected every 3 s. Representative cells are shown in *E*. (*F*) Peak $LimE_{\Delta coil}$-RFP accumulation at the cortex of individual cells was quantified as the inverse of the mean cytoplasmic intensity 6 s after the start of stimulation, normalized for time 0. Horizontal lines and error bars represent mean ± SD, $*P < 0.05$, $**P < 0.01$. (*G*) WT or *gpgA*⁻ cells migrating in the absence or presence of flow were imaged every 15 s for 15 min. Tracks of 50 cells are shown. Arrowheads point to areas of biosensor accumulation at the cortex. (Scale bar, 10 μm.)

of responses to acute mechanical stimulation delivered by unidirectional laminar flow, the peak response of Pkd2-null or Mcln-null cells was not significantly different from WT cells (Fig. 5*E* and Movie S13). Furthermore, we disrupted the gene for the *Dictyostelium* homolog of a mechanosensitive cation channel Piezo (16), and assessed PKBR1 and ERK2 phosphorylation, as well as $LimE_{\Delta coil}$ recruitment following acute mechanical stimulation (Fig. S5 *E–G*). Neither response was significantly impaired in piezo-null compared with WT cells.

In contrast, cells lacking IP3 receptor homolog IplA showed a significantly weaker $LimE_{\Delta coil}$ recruitment following acute exposure to unidirectional flow (Fig. 5 *E* and *F*, Fig. S5*D*, and Movie S14). Consistent with previous observations of IplA-null cells, high concentrations of extracellular calcium partially rescued the response (Fig. 5*F*, Fig. S5*D*, and Movie S14) (17). The peak $LimE_{\Delta coil}$ recruitment significantly improved by ∼8% in 10 mM $CaCl_2$ compared with 0.2 mM ($P < 0.05$).

Role of the Cytoskeleton in the Response to Acute Mechanical Stimulation. Because the actin cytoskeleton has been implicated in mechanosensation, we examined whether it is required for transmitting the acute mechanical stimulus to the cell. Inhibition of actin polymerization with 5 μM latrunculin A (LatA) abolished recruitment of RBD-GFP to the cell cortex following acute stimulation with unidirectional shear flow (Fig. 6*A* and Movie S15). The average peak response of RBD-GFP 6 s after stimulation was significantly reduced from almost 20% compared with basal values to 0 ($P < 0.001$) in vehicle vs. LatA-treated cells

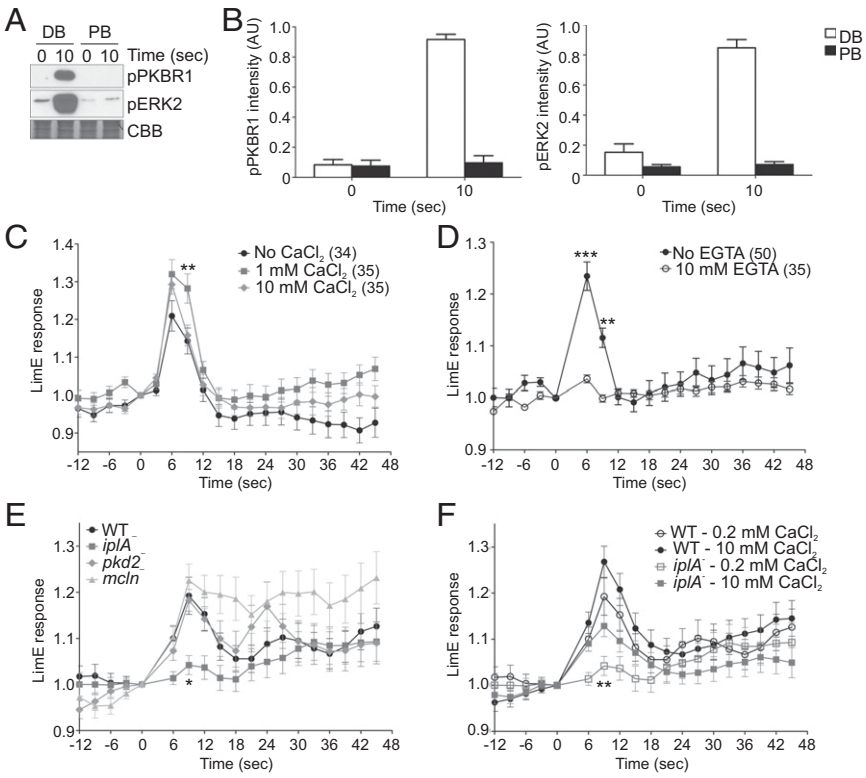

Fig. 5. Role of cations and cation channels in the response to acute mechanical stimulation. (*A* and *B*) Aggregation-competent WT cells in phosphate buffer (PB) or PB supplemented with 2 mM $MgSO_4$ and 0.2 mM $CaCl_2$ [developmental buffer (DB)] were stimulated on a rotary shaker for 5 s, lysed at the indicated time points, and immunoblotted with antibodies that recognize phosphorylated PKBR1 and ERK2. The membrane was stained with CBB to show equal protein loading. A representative immunoblot is shown in *A*. (*B*) Mean intensity of phospho-PKBR1 and phospho-ERK2 bands was normalized for the integrated intensity of 0- and 10-s DB bands. Values are mean ± SE of four independent experiments. (*C* and *D*) Vegetative WT cells expressing $LimE_{\Delta coil}$-RFP were kept in tricine buffer, treated with the indicated concentrations of $CaCl_2$ for at least 5 min (*C*) or with 10 mM EGTA or vehicle for at least 30 min (*D*) and then stimulated with unidirectional laminar flow at 41 dyn/cm^2 for 2 s. Images were collected every 3 s. $LimE_{\Delta coil}$-RFP accumulation at the cortex was quantified as in Fig. 1*F*. Values are mean ± SE. The number of cells analyzed is indicated beside each condition. Peak response values for individual cells are shown in Fig. S5 *B* and *C*. (*E* and *F*) Vegetative WT, *iplA*$^-$, *pkd2*$^-$, or *mcln*$^-$ cells expressing $LimE_{\Delta coil}$-RFP were kept in tricine buffer supplemented with 0.2 mM $CaCl_2$ (*E* and *F*) or 10 mM $CaCl_2$ (*F*), and then stimulated with unidirectional laminar flow, imaged, and analyzed as in *C*. Values are mean ± SE of 30 cells. Peak response values for individual cells in *F* are shown in Fig. S5*D*. *$P < 0.05$, **$P < 0.01$, ***$P < 0.001$ compared with WT or vehicle control, unless indicated otherwise.

(Fig. 6 *A* and *B* and Fig. S6*A*). $LimE_{\Delta coil}$ recruitment was also completely blocked in LatA-treated cells, confirming complete inhibition of actin polymerization following LatA treatment. The 5-μM LatA treatment also inhibited phosphorylation of PKBR1 and ERK2 at 10 and 30 s after 5-s mechanical stimulation with a rotary shaker (Fig. 6 *C* and *D*). The inhibitory effect of LatA was dose dependent (Fig. S6*B*). Cells treated with LatA retained their ability to respond to chemoattractant. Treatment with 100 μM folic acid or 1 μM cAMP led to an increase in cortical RBD localization and PKBR1 and PKBA phosphorylation in vegetative and aggregation-competent cells, respectively (Fig. S6 *C* and *D*). In contrast to the strong requirement for polymerized actin, there did not appear to be a requirement for myosin II because cells lacking myosin II were capable of generating a robust response when stimulated on a rotary shaker or with unidirectional flow (Fig. 6*E* and Fig. S6 *E* and *F*).

We also tested whether disruption of other structural components would inhibit response to acute mechanical stimulation. Treatment of cells with up to 50 μM benomyl, a drug that destabilizes microtubules, did not abolish recruitment of RBD or $LimE_{\Delta coil}$ to the cortex following a brief pulse of flow (Fig. 6 *F* and *G* and Fig. S6 *G* and *H*, and Movie S16). We also examined effects of benomyl on the phosphorylation of PKBR1 and ERK2 following acute stimulation on a rotary shaker (Fig. S6 *I*–*K*). Benomyl did not block stimulation-induced phosphorylation (Fig. S6 *I* and *J*). It should be noted that benomyl dramatically reduced the amount of basal phosphorylation in a dose-dependent manner (Fig. S6*K*), which introduced error into the calculation of the fold increase in phosphorylation. Thus, it appears that an intact microtubule scaffold modulates the basal activity but unlike the actin cytoskeleton its effects can be overridden by a strong mechanical stimulus.

Discussion

We found that brief stimulation of cells with shear flow results in rapid transient activation of all tested signal transduction pathways, as well as actin polymerization, similarly to uniform stimulation with a chemoattractant (Fig. 7). We observed simultaneous changes in the activity and/or localization of molecules from multiple parallel pathways in the chemotactic signaling network, including ERK2, Ras GTPases, Rap1, KrsB, PKBR1, PIP3, PKBA, PTEN, and CynA. The kinetics of these changes matched those triggered by chemoattractant. As they do when stimulated with chemoattractants, cells respond to increments in mechanical force in a saturable manner. Saturating stimuli trigger all-or-none responses followed by a refractory period, during which the system does not respond to any stimulus of comparable strength. These properties suggest that, remarkably, mechanical stimuli feed into the same excitable network previously delineated for chemoattractants. For chemoattractants, the signal

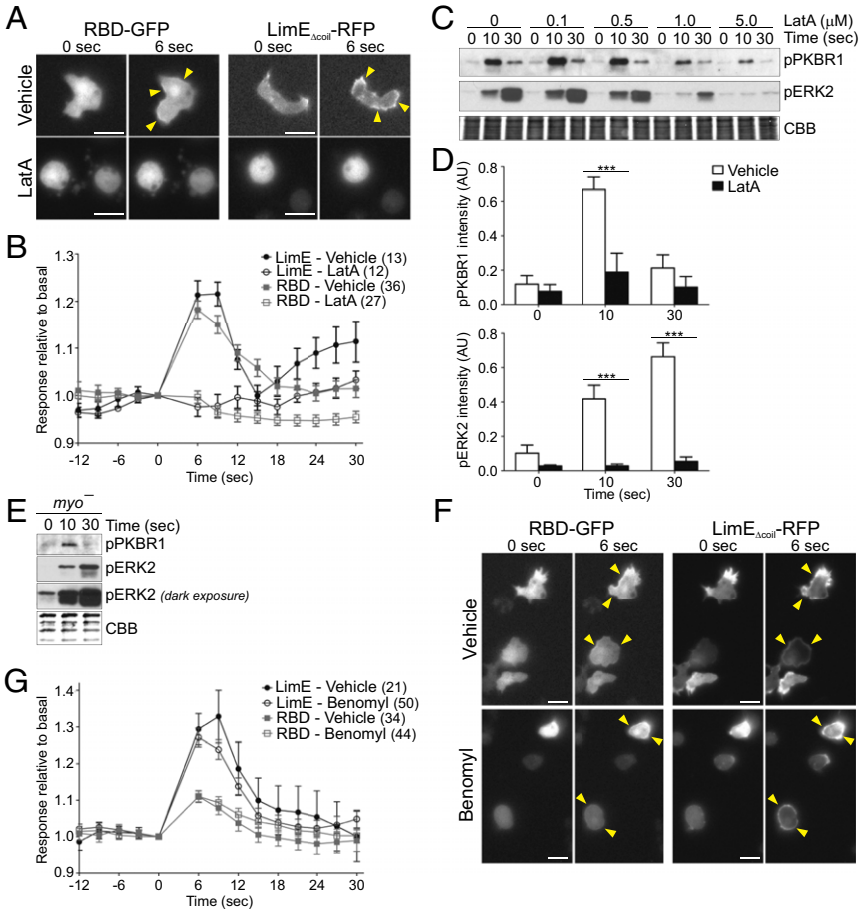

Fig. 6. Role of the cytoskeleton in the response to acute mechanical stimulation. (*A* and *B*) Vegetative WT cells expressing LimE$_{\Delta coil}$-RFP or RBD-GFP were treated with vehicle or 5 μM LatA for at least 15 min, and then stimulated with unidirectional laminar flow at 41 dyn/cm^2 for 2 s. Images were collected every 3 s. Representative cells are shown in *A*. (*B*) RBD-GFP and LimE$_{\Delta coil}$-RFP accumulation at the cortex was quantified as in Fig. 1*F*. Values are mean ± SE. The number of cells analyzed is indicated beside each condition. Peak response values for individual cells are shown in Fig. S6*A*. (*C* and *D*) Aggregation-competent WT cells were pretreated with LatA for 30 min, stimulated on a rotary shaker for 5 s, lysed at the indicated time points, and immunoblotted using antibodies that recognize phosphorylated PKBR1 or ERK2. The membrane was stained with CBB to show equal protein loading. A blot representative of three independent experiments is shown in *C* and quantified in Fig. S6*B*. (*D*) The mean intensity of the phosphorylated bands for vehicle and 5 μM LatA was normalized for the integrated intensity of 0-, 10-, and 30-s vehicle bands. Values are mean ± SE of 5 (pPKBR1) and 6 (pERK2) independent experiments. (*E*) Aggregation-competent *myo*$^-$ cells were stimulated on a rotary shaker for 5 s, lysed, and immunoblotted as in *C*. A blot representative of at least two independent experiments is shown. (*F* and *G*) Vegetative WT cells expressing LimE$_{\Delta coil}$-RFP or RBD-GFP were treated with vehicle or 50 μM benomyl for at least 20 min and then stimulated with unidirectional laminar flow at 41 dyn/cm^2 for 2 s. Images were collected every 3 s. Representative cells are shown in *F*. (*G*) RBD-GFP and LimE$_{\Delta coil}$-RFP accumulation at the cortex was quantified as the inverse of the mean cytoplasmic intensity normalized for time 0. Values are mean ± SE. The number of cells analyzed is indicated beside each condition. Peak response values for individual cells are shown in Fig. S6*F*. ***$P < 0.001$. Arrowheads point to areas of biosensor accumulation at the cortex. (Scale bar, 10 μm.)

enters through a receptor/G protein network, which biases an excitable signal transduction network, which drives the cytoskeleton network. The convergence of chemical and mechanical stimuli on the signal transduction network would allow the cell to integrate the inputs. For mechanical perturbation, we have identified several components that are required, including polymerized actin, calcium, and G protein βγ subunits, as well as the overall activity of the signal transduction network. Thus, rather than pointing to entry through a specific network, our data suggest that the responsiveness to mechanical stimuli may be able to enter through any of the networks.

We observed virtually complete inhibition of the response to mechanical perturbation in cells with depolymerized actin cytoskeleton, suggesting that an intact actin cytoskeleton is required for the transmission of the mechanical stimulus to the signal transduction network. The requirement of an intact cytoskeleton is specific for the mechanical stimulus because cells treated with latrunculin do respond to chemoattractants (Fig. S6 *C* and *D*) (18, 19). The response was independent of overall cytoskeletal architecture because depolymerizing the microtubule network did not significantly affect the response to mechanical stimulation. It is known that cells treated with latrunculin have greatly decreased cortical tension, which may be important for the mechanoresponse (20).

Depletion of calcium or disruption of IplA blocked the response suggesting that it is mediated by the activity of mechanosensitive cation channels or it may require a general rise in cytosolic calcium. Biochemical responses to mechanical stimuli have been attributed to mechanosensitive cation channels, including transient receptor potential (TRP) channels such as polycystin-2 (Pkd2), as well as piezo channels (21). Pkd-2 and another TRP family channel mucolipin (Mcln) have been implicated in shear-flow–induced migration of *Dictyostelium* cells (15). We identified and disrupted a homolog of piezo. However, in our assays the peak response to acute mechanical stimulation was not noticeably changed in cells lacking any of these putative

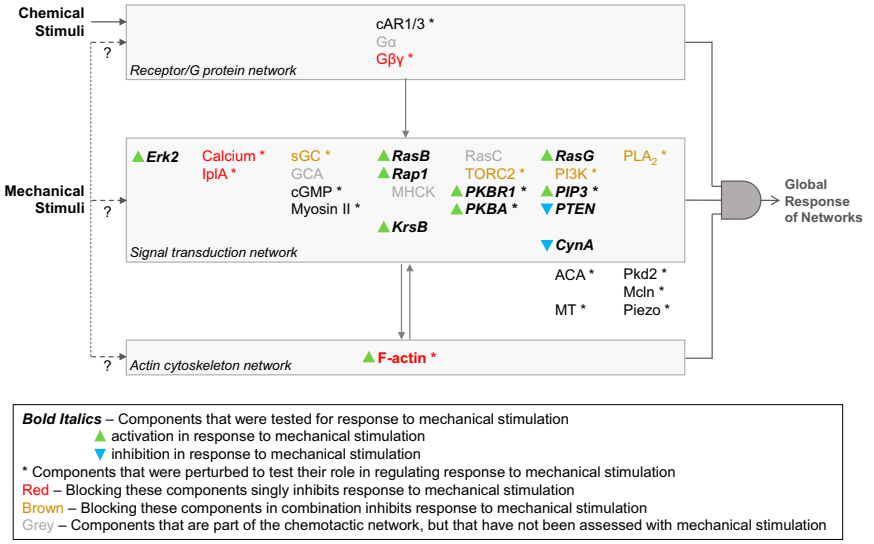

Fig. 7. Activation of the chemotactic signaling network by chemical and mechanical stimuli. Background: Chemoattractants bind to GPCRs, which leads to dissociation and activation of G protein α and βγ subunits. This signal is further amplified by multiple parallel pathways within the signal transduction network, which is required for biased actin polymerization. In response to chemoattractant, most of the molecules within the signal transduction network are transiently activated or recruited to the cortex, although PTEN and CynA dissociate from the cortex. In this report: First, multiple nodes (shown in bold italics) within the chemotactic signal transduction and cytoskeletal networks were tested in response to acute mechanical stimulation. Eight either accumulated at the cortex or displayed activating phosphorylation (green triangles), and two lost cortical localization (blue triangles), all with the same dynamics as for chemoattractants. Second, tests were repeated after numerous components (marked with *) implicated in chemotactic responses, mechanotransduction, and cytoskeletal integrity were perturbed using genetic deletions and/or pharmacological inhibitors. Because perturbations within all three networks inhibited the response to acute mechanical stimulation (shown in red and brown), it appears that all three networks coordinate in a logical AND gate-type manner to produce a global response. The possible point(s) of entry of the mechanical stimuli is discussed in the text.

mechanosensitive channels, although it is possible that the mutants would show altered responsiveness under other conditions (e.g., different flow rates, calcium concentrations, or substrates). Another possibility is that there is functional redundancy between different mechanosensitive channels as has been postulated for bacterial Msc channels (22). It would be interesting to examine cells with combined deletion of two or more channels. In addition, both *pkd2*$^-$ and *mcln*$^-$ cells appeared to have some differences in the actin response following the initial peak. The inability to mount a directional response could potentially explain aberrant migration of these cells even if the initial response is robust, although this was not addressed in the current study. Taken together, these results suggest that the response to mechanical stimuli requires a general calcium flux that is likely mediated by IplA. Whether specific mechanosensitive channels are involved in this acute response remains an open question.

Perhaps somewhat surprising was the observation that the response to acute mechanical stimulation was reduced in cells that lack either β or γ subunits of G proteins. In contrast, cells lacking both of the major chemoattractant receptors cAR1 and cAR3 were still responsive. In addition, it is unlikely that soluble factors binding to another GPCR mediate the response because cells in perfusion were still able to respond to shear force. Nevertheless, it is possible that G proteins are directly involved in the conversion of a mechanical stimulus to a biochemical response. In fact, purified G proteins in phospholipid vesicles were activated in response to acute shear stress in the absence of other protein components (23). However, cells lacking β or γ subunits of G proteins migrate more slowly randomly, in chemotaxis, electrotaxis, and shear flow, and are deficient in phagocytosis, suggesting that the defect in mechanosensitivity might be related to the decreased baseline activity (13, 24–26).

The fact that perturbations of multiple networks all inhibit the response suggests that the mechanical stimulus may enter at multiple points or that changes that affect the basal activation state of the excitable signal transduction network might also affect the sensitivity to mechanical stimuli. Indeed, perturbations within the signal transduction network itself reduced the response to mechanical stimulation. As noted above, depletion of calcium blocked the response. Furthermore, we observed pronounced inhibition (~60%) in cells that lack activity in four parallel pathways (sGC, PLA_2, Pia, and PI3K). These perturbations correlated with the greatly diminished random migration of these cells (Fig. 4) (8, 27). Perturbation of other networks, by disrupting G proteins or actin cytoskeleton, also affected the apparent excitability of the signal transduction network (8, 9, 28). Even if a stimulus entered at one point, for example through actin cytoskeleton, the activation of the signal transduction network could be required to amplify the signal. Because the signal transduction network is excitable, its activation requires crossing of a threshold, and any perturbation that raises the threshold would be expected to limit the amplification. Inherent variation in the basal activation state of individual cells also likely explains the variation in the response observed in Fig. 1 *F* and *G*.

The activation of the signal transduction and cytoskeletal networks in response to acute shear stress stimulus is not simply a consequence of cells migrating under continuous flow, but is likely a prerequisite for this mode of directed migration. When cells are stimulated with shear flow for 10 s, the peak response is observed before the end of the stimulus and is followed by a transient pause in migration. Furthermore, continuous exposure to flow first induces a transient burst in the activation of the signal transduction and cytoskeletal networks, followed by a directional response and migration. This series of events is analogous to the response of a cell when first exposed to a gradient of chemoattractant. It also shows a uniform response, which is later followed by a polarized response in the direction of the gradient.

The series of events outlined above might explain shear-flow–induced migration against the flow. We and others observe migration of WT cells against the flow at lower shear stress levels, whereas at higher shear stress levels cells begin migrating in the direction of the flow (4, 13). Migration against the flow might occur if shear flow stimulates the signal transduction network and actin polymerization preferentially at the leading edge of the cell. Consistently, G-protein–null cells, which failed to respond to acute mechanical stimulation under the typical conditions, were deficient in migrating against the flow, but could migrate with the flow. This suggests that migration with the flow does not depend on the acute response. Cells migrating with the flow show leading edge markers, such as PIP3, at the front of the cell (7), but this is likely a consequence of there being more pseudopods in the direction of migration. It is important to note that the shear stress values that induced migration either against or with flow were both sufficient for the induction of the acute

response. In fact, even though based on the dose curve low shear stress values that were used for migration analysis do not induce a full response, when the stimulation is continuous, the transient response likely approaches saturation as seen from Fig. 3*A* (2- vs. 10-s response at 15 dyn/cm^2). It is also worth noting that the defects in shear-flow–induced migration of cells lacking Pkd2 or Mcln, which were not defective in our assay, were reported under relatively high shear flow conditions (15). Overall, the possibility that migration against or with the flow involves distinct mechanisms is intriguing and warrants further study.

So far very few studies have addressed how different external stimuli are processed and whether there is integration of various inputs. Li et al. examined migration of T cells in the presence of an electric field and an opposing chemoattractant gradient (29). In their study, the cells continued migrating with the same speed toward the cathode, although their directionality was significantly impaired by the opposing chemoattractant gradient. This finding is consistent with our model where different stimuli are integrated together at the level of the signal transduction network, and thus the overall response depends on the relative strength of the two stimuli. Although technically challenging, future studies should assess the behavior of cells that are simultaneously exposed to shear flow and a chemoattractant gradient.

The response to acute mechanical stimulation appears to be a conserved phenomenon, at least among cells undergoing amoeboid migration. Similarly to *Dictyostelium*, neutrophils and T lymphocytes have also been previously reported to directionally migrate in response to shear flow (30, 31). However, whether the acute response that was observed in human neutrophils in this study is a prerequisite for shear flow-induced migration as it is in *Dictyostelium* remains to be examined. We hypothesize that the response to acute mechanical stimulation observed in this study is not specific to shear flow, but likely represents a response to any mechanical perturbation. Both *Dictyostelium* and mammalian migratory cells are constantly exposed to physical cues as they move through 3D matrices in the soil or interstitial space, respectively, and these signals likely integrate with other directional cues to guide cell migration.

Our study demonstrates that an acute mechanical stimulus directly activates a vast array of molecules in the chemotactic signal transduction and actin cytoskeleton networks. Most studies of shear-flow–directed migration have examined cells under steady-state conditions, and this response to the initial application of shear flow has not been observed. We propose that a common signal transduction network underlies responses not only to chemical and mechanical stimuli, but also to other external inputs, for example changes in electric fields, although this remains to be tested.

Materials and Methods

A detailed description of materials and methods is provided in *SI Materials and Methods*.

ACKNOWLEDGMENTS. We thank Drs. Pierre Cosson, Peter J. van Haastert, Yoichiro Kamimura, Robert R. Kay, Arjan Kortholt, Douglas N. Robinson, and Masahiro Ueda, as well as dictyBase for providing expression constructs and strains used in this study, and members of the P.N.D. laboratory for helpful suggestions and discussion. This work was supported by NIH Grant R35 GM118177 (to P.N.D.).

1. Stroka KM, Konstantopoulos K (2014) Physical biology in cancer. 4. Physical cues guide tumor cell adhesion and migration. *Am J Physiol Cell Physiol* 306(2):C98–C109.
2. Cortese B, Palamà IE, D'Amone S, Gigli G (2014) Influence of electrotaxis on cell behaviour. *Integr Biol (Camb)* 6(9):817–830.
3. Artemenko Y, Lampert TJ, Devreotes PN (2014) Moving towards a paradigm: Common mechanisms of chemotactic signaling in Dictyostelium and mammalian leukocytes. *Cell Mol Life Sci* 71(19):3711–3747.
4. Dalous J, et al. (2008) Reversal of cell polarity and actin-myosin cytoskeleton reorganization under mechanical and chemical stimulation. *Biophys J* 94(3):1063–1074.
5. Sato MJ, et al. (2009) Switching direction in electric-signal-induced cell migration by cyclic guanosine monophosphate and phosphatidylinositol signaling. *Proc Natl Acad Sci USA* 106(16):6667–6672.
6. Zhao M, Pu J, Forrester JV, McCaig CD (2002) Membrane lipids, EGF receptors, and intracellular signals colocalize and are polarized in epithelial cells moving directionally in a physiological electric field. *FASEB J* 16(8):857–859.
7. Décave E, et al. (2003) Shear flow-induced motility of Dictyostelium discoideum cells on solid substrate. *J Cell Sci* 116(Pt 21):4331–4343.
8. Huang CH, Tang M, Shi C, Iglesias PA, Devreotes PN (2013) An excitable signal integrator couples to an idling cytoskeletal oscillator to drive cell migration. *Nat Cell Biol* 15(11):1307–1316.
9. Tang M, et al. (2014) Evolutionarily conserved coupling of adaptive and excitable networks mediates eukaryotic chemotaxis. *Nat Commun* 5:5175.
10. Kortholt A, et al. (2011) Dictyostelium chemotaxis: Essential Ras activation and accessory signalling pathways for amplification. *EMBO Rep* 12(12):1273–1279.
11. Veltman DM, Keizer-Gunnik I, Van Haastert PJM (2008) Four key signaling pathways mediating chemotaxis in Dictyostelium discoideum. *J Cell Biol* 180(4):747–753.
12. Veltman DM, Lemieux MG, Knecht DA, Insall RH (2014) PIP_3-dependent macropinocytosis is incompatible with chemotaxis. *J Cell Biol* 204(4):497–505.
13. Fache S, et al. (2005) Calcium mobilization stimulates Dictyostelium discoideum shear-flow-induced cell motility. *J Cell Sci* 118(Pt 15):3445–3457.
14. Munaron L (2011) Shuffling the cards in signal transduction: Calcium, arachidonic acid and mechanosensitivity. *World J Biol Chem* 2(4):59–66.
15. Lima WC, Vinet A, Pieters J, Cosson P (2014) Role of PKD2 in rheotaxis in Dictyostelium. *PLoS One* 9(2):e88682.
16. Coste B, et al. (2010) Piezo1 and Piezo2 are essential components of distinct mechanically activated cation channels. *Science* 330(6000):55–60.
17. Lusche DF, et al. (2012) The IplA Ca2+ channel of Dictyostelium discoideum is necessary for chemotaxis mediated through Ca2+, but not through cAMP, and has a fundamental role in natural aggregation. *J Cell Sci* 125(Pt 7):1770–1783.
18. Postma M, et al. (2004) Sensitization of Dictyostelium chemotaxis by phosphoinositide-3-kinase-mediated self-organizing signalling patches. *J Cell Sci* 117(Pt 14):2925–2935.
19. Janetopoulos C, Ma L, Devreotes PN, Iglesias PA (2004) Chemoattractant-induced phosphatidylinositol 3,4,5-trisphosphate accumulation is spatially amplified and adapts, independent of the actin cytoskeleton. *Proc Natl Acad Sci USA* 101(24):8951–8956.
20. Srivastava V, Robinson DN (2015) Mechanical stress and network structure drive protein dynamics during cytokinesis. *Curr Biol* 25(5):663–670.
21. Ranade SS, Syeda R, Patapoutian A (2015) Mechanically activated ion channels. *Neuron* 87(6):1162–1179.
22. Booth IR, Miller S, Müller A, Lehtovirta-Morley L (2015) The evolution of bacterial mechanosensitive channels. *Cell Calcium* 57(3):140–150.
23. Gudi SR, Clark CB, Frangos JA (1996) Fluid flow rapidly activates G proteins in human endothelial cells. Involvement of G proteins in mechanochemical signal transduction. *Circ Res* 79(4):834–839.
24. Zhao M, Jin T, McCaig CD, Forrester JV, Devreotes PN (2002) Genetic analysis of the role of G protein-coupled receptor signaling in electrotaxis. *J Cell Biol* 157(6):921–927.
25. Wu L, Valkema R, Van Haastert PJ, Devreotes PN (1995) The G protein beta subunit is essential for multiple responses to chemoattractants in Dictyostelium. *J Cell Biol* 129(6):1667–1675.
26. Peracino B, et al. (1998) G protein beta subunit-null mutants are impaired in phagocytosis and chemotaxis due to inappropriate regulation of the actin cytoskeleton. *J Cell Biol* 141(7):1529–1537.
27. Schaloske RH, et al. (2005) Ca2+ regulation in the absence of the iplA gene product in Dictyostelium discoideum. *BMC Cell Biol* 6(1):13.
28. Taniguchi D, et al. (2013) Phase geometries of two-dimensional excitable waves govern self-organized morphodynamics of amoeboid cells. *Proc Natl Acad Sci USA* 110(13):5016–5021.
29. Li J, Zhu L, Zhang M, Lin F (2012) Microfluidic device for studying cell migration in single or co-existing chemical gradients and electric fields. *Biomicrofluidics* 6(2): 024121–024113.
30. Phillipson M, et al. (2009) Vav1 is essential for mechanotactic crawling and migration of neutrophils out of the inflamed microvasculature. *J Immunol* 182(11):6870–6878.
31. Valignat M-P, Theodoly O, Gucciardi A, Hogg N, Lellouch AC (2013) T lymphocytes orient against the direction of fluid flow during LFA-1-mediated migration. *Biophys J* 104(2):322–331.
32. Artemenko Y, Swaney KF, Devreotes PN (2011) Assessment of development and chemotaxis in Dictyostelium discoideum mutants. *Methods Mol Biol* 769:287–309.
33. Insall RH, Soede RD, Schaap P, Devreotes PN (1994) Two cAMP receptors activate common signaling pathways in Dictyostelium. *Mol Biol Cell* 5(6):703–711.
34. Pitt GS, et al. (1992) Structurally distinct and stage-specific adenylyl cyclase genes play different roles in Dictyostelium development. *Cell* 69(2):305–315.
35. Ruppel KM, Uyeda TQ, Spudich JA (1994) Role of highly conserved lysine 130 of myosin motor domain. In vivo and in vitro characterization of site specifically mutated myosin. *J Biol Chem* 269(29):18773–18780.
36. Swaney KF, Borleis J, Iglesias PA, Devreotes PN (2015) Novel protein Callipygian defines the back of migrating cells. *Proc Natl Acad Sci USA* 112(29):E3845–E3854.
37. Kortholt A, et al. (2010) A Rap/phosphatidylinositol 3-kinase pathway controls pseudopod formation [corrected]. *Mol Biol Cell* 21(6):936–945.
38. Artemenko Y, et al. (2012) Tumor suppressor Hippo/MST1 kinase mediates chemotaxis by regulating spreading and adhesion. *Proc Natl Acad Sci USA* 109(34):13632–13637.
39. Schindelin J, et al. (2012) Fiji: An open-source platform for biological-image analysis. *Nat Methods* 9(7):676–682.
40. Wang MJ, Artemenko Y, Cai WJ, Iglesias PA, Devreotes PN (2014) The directional response of chemotactic cells depends on a balance between cytoskeletal architecture and the external gradient. *Cell Reports* 9(3):1110–1121.